Received 28 September 2022 | Revised 20 November 2022 | Accepted 05 December 2022
Vol. 03, No. 02,13 pages

RESEARCH ARTICLE TUJES Tobruk University Journal of Engineering Sciences

Performance Investigation of 5 GHz Fixed Wireless Access Network

Ali O. Gliwan[1], Wisam M. Eltarjaman[2], and Hisham B. Almelah[3]

[1] Electrical and Electronic, Misurata University, Misurata, Libya
[2] Computer Science, Misurata University, Misurata, Libya
[3] Electrical and Electronic, Misurata University, Misurata, Libya
Ali.gliwan@eng.misuratau.edu.ly.com

Abstract. Fixed Wireless Access (FWA) networks made substantial progress in providing reliable wireless services for users everywhere. To the best of our knowledge, this is the first attempt in Libya to study and assess the performance of a realistic local FWA network operating on an unlicensed 5 GHz band despite the widespread networks of this type throughout the country. This paper provides a detailed analysis of several factors and measurements that affect network performance. The study depends on measurements extracted from a real dataset of an active FWA network. The central performance metric we consider is the capacity offered by the network to the subscribers. Using modern and powerful Python libraries, we present statistical summaries for those factors to estimate the impact of each one individually on the performance. Finally, we utilized the well-known free space Path Loss (PL) model behavior to demonstrate and validate the accuracy of our measurements.

Keywords: FWA, 5 GHz, WISP, Libya.

1 Introduction

The wired network in Libya suffered numerous obstacles because of its antiquity. Examples are limited reachability to end users, lack of follow-up and maintenance, and several other technical problems. Those obstacles, collectively, made the regional wired network unable to cope with the rapid growth in demand for broadband Internet services. As a result, the easier-to-spread and less expensive wireless networks represent a successful and promising alternative solution to provide equivalent communication services to those the traditional fixed-line broadband networks (e.g., DSL or cable modem [1]) can provide. Wireless networks excel, especially in suburban areas, which do not have the sufficient infrastructure of copper or optical fiber cables to support wired broadband services. Also, wireless networks represent a good alternative for the regions where the wired network is underperforming or insufficient to meet the customers' needs.

Technologies called Wireless to The Home (WTTH) provide wireless Internet services to headquarters, such as homes and companies, using several wireless standards. Examples of these standards include IEEE 802.16 [2] for the Worldwide Interoperability for Microwave Access (WiMAX) technology and IEEE 802.11 [3] for Wi-Fi versions, and recently Long-Term Evolution (LTE) or so-called 4G technology [4]. These networks fall in the FWA networks category [3]. FWA is a broadband wireless access system that significantly improves the system's capacity (which is commonly used in the digital communication sector

as a representation of the link speed) and provides high throughput, broad coverage, and reliable service efficiency and security [3].

Most of the Wireless Internet Service providers (WISP) networks, as seen in Fig. 1, follow a typical FWA system with a minimum of three Access Point (AP) units, often installed on high towers, so that a large number of subscribers can reach these APs. The access units are connected wirelessly to the Customer Premises Equipment (CPE) at the subscriber property, which connects to routers to obtain broadband wireless signal [1]. Successful distribution of APs requires careful and professional planning to reduce propagation PL caused by the hosting environment of service areas, thus obtaining the required service efficiency.

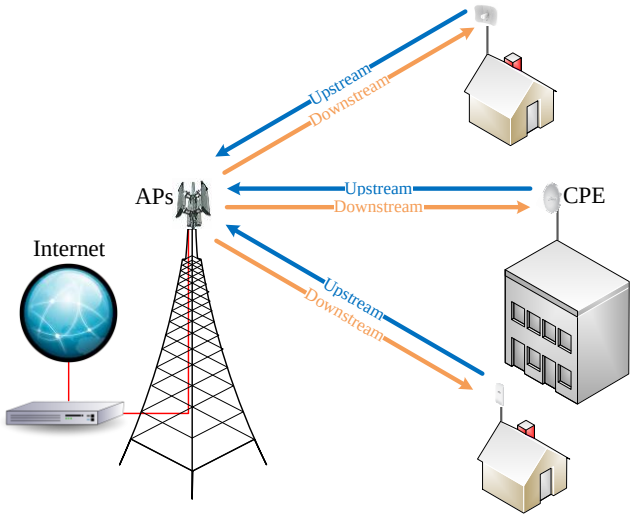

Fig. 1. Simplified WISP Network.

This work represents the first step in a research plan to address the challenges expected when using FWA technology. The system examined in this paper is an FWA system in the 5 GHz Industry Scientific Medical (ISM) bands. Ubiquiti's [5] Time Division Multiple Access (TDMA) airMAX ac protocol shares the air interface between the users, which allows each subscriber to send and receive data via predesignated time slots scheduled by a smart controller installed in the AP.

We study and analyze data for nearly one thousand subscribers within a local Internet Service Provider (ISP) network operating in Misurata city as a realistic model for the FWA network. The study relies on a real dataset aggregated and summarized as relationships through which we evaluate the network performance and propose practical solutions to the discovered problems. Following is a summary of the main tasks accomplished in this work:

1. **Data compilation** Collect, arrange, and schedule a large amount of data for an existing local WISP network. Then, analyze the data using statistical Python libraries to obtain "useful" empirical results for many network parameters.
2. **Analysis and presentation** Present the results for real-life FWA deployment measurements and emphasize "important" relationships between network parameters.
3. **Results confirmation** Validate the accuracy of the free space PL model on the compiled datasets.

The rest of this paper is structured as follows. We reviewed the related works in Section 2 to align our work with the literature. Section 3 illustrates the layout of the case study network. In Section 4, we talked about the collected measurements from our network. A statistical presentation of network performance parameters was given in Section 5 to evaluate the effect of each of these parameters on the performance quality. Finally, we conclude this paper in section 6.

2 Related work

Since WiFi technology represents the typical choice for indoor applications [6], we see adequate research in the literature focusing on the PL problem. For instance, [6-9] proposed different mathematical models to approximate the signal's power loss as a function of the propagation distance of that signal under various parameters. Recently, attention has been drawn toward WiFi-based long-range systems to treat the issues mentioned above in the introduction. Accordingly, many studies focused on the effect of specific climatic and environmental conditions, frequency bands, antenna height, and dynamic distances on PL models[8, 10-16]. Few of these studies included measurements from real datasets, while the rest were just simulation-based.

More relevant works to the present paper are found in [1], [2], and [3]. The Authors in [1] contribute by modifying some PL models so they can fit the 5G FWA system. The paper suggested and used a flavor of Monte-Carlo simulation to validate that modified model and then evaluated PL and capacity using that simulation. While [2] presented some measurement results for a fixed WiMAX network and derived an analytical PL model based on those empirical results. On the other hand, [3] proposed a new empirical PL model. They tested and validated their model on many datasets collected from different environments.
Recently, FWA [17, 18] received the major attraction to accommodate the 5G demand and replace the high cost of the fiber networks [1, 19, 20]. Quite an amount of research in the literature has focused on access technology: Global System for Mobile (GSM) [10, 21] and empirical propagation PL models for mobile communication [22-24], WiMAX [2, 10, 25], and the effect of PL in different frequencies and conditions, LTE [14, 26, 27] with different frequency bands, or the co- existing of LTE with WiFi [4]. [3, 28-30] investigated the network performance in an unlicensed 5 GHz frequency band concentrating on PL impact. Intensive work in [19, 27, 31-33] studied the network performance in the urban environment; [31, 33] focused, particularly, on the suburban environment. In this work, however, we focus on the performance analysis of the outdoor TDMA FWA unlicensed 5 GHz broadband frequency for wireless networks in suburban areas.

3 System Description

The network examined in this paper is an FWA network operating in the 5 GHz frequency band, particularly between 4.9 GHz and 5. This network includes 70 wireless APs distributed on 15 sites/towers, providing services to 1000 active subscribers' CPEs. Each AP operates in Point-to-Multi-Point (P2MP) mode with Global Positioning System (GPS) synchronized clock TDMA and utilizes a 20 MHz shared channel between both the upstream and downstream Each AP connects to a sector antenna with a 90˚ beamwidth using one frequency. As seen in **Table 1**, the system has four different AP models; each AP has its explicit configuration. The height range of the system APs altitude is between (68m-102m) from Mean Sea Level (MSL).

Table 1. The specifications for the APs used in the Network.

Rocket Model	90o Sector Antenna Gain (dBi)	Pt (dBm)	MIMO	Freq. Band (GHz)	Ch. Width (MHz)
R5AC-Lite	20	27	Yes	5	20
R5AC-PTMP	20	27	Yes	5	20
R5AC-PRISM	22	27	Yes	5	20
RP-5AC-Gen2	22	28	Yes	5	20

The CPEs are fixed antennas usually located outdoors on the roof of a house or a building (the minimum recommended height is 10 m from the ground). A CPE must be in the Line-of-Sight (LoS) of the nearest AP,

and the maximum permissible distance is 7 Km. **Table 2** shows the different CPEs models used in the network and their specifications.

Table 2. The network used CPEs specifications.

Rocket Model	90o Sector Antenna Gain (dBi)	Pt (dBm)	MIMO	Freq. Band (GHz)	Ch. Width (MHz)
LBE-5AC-23	23	24	Yes	5	20
LBE-5AC-16-120	16	25	Yes	5	20
LBE-5AC-Gen2	23	28	Yes	5	20
LBE-M5-23	23	25	No	5	20
NBM5-22	22	23	Yes	5	20
PBE-5AC-Gen2	25	24	Yes	5	20
PBE-M5-300	22	26	Yes	5	20
PBE-M5-400	25	26	Yes	5	20

The area of deployment consists of Misrata city (the third city in Libya population-wise) with a population of 450.000, where the population density is low in the suburban areas outside the town center and denser in the town center with tall buildings (on average the height is 4 floors).
There are more than five other WISPs in Misrata city using the same 5 GHz frequency band, which means more than 200 sites, with an average of 5APs per site [34]. Absent of an arrangement policy for frequency sharing and allocation between those WISPs leads to spectrum interference, particularly in dense areas, i.e., the town center.

4 Network Measurements

This paper used an empirical research method for analysis performed over measurement data extracted from an FWA system deployed in real life. Our network uses Ubiquiti Network Management System (UMS) to manage APs and CPEs. Using UMS, the operator can configure various control parameters for APs and CPEs, e.g., the operating frequency, channel bandwidth, and maximum transmission power. The operator also can monitor, in real-time, different network performance attributes, e.g., downstream and upstream capacity and throughput of each CPE and AP, the transmission modulation technology, the transmitted power and the receiver sensitivity for both AP and network CPEs, the Signal to Noise Ratio (SNR), and most importantly the noise margin for the whole frequency band. Since the system operator visualizes the frequency interference in real time, he can adjust the AP's operating frequency to lower the interference. All needed performance attributes have been collected on the same date (May 15, 2022) to ensure identical conditions among all network elements. We assemble the entire dataset in one CSV file. We use Python numeric and math plotting libraries for the visual data analysis presented in Section **5**.

5 Network Performance Analysis

We shall consider the capacity that a subscriber can get as the measure of the network performance. So, we start our discussion by looking at the distribution of the network's upstream and downstream capacity to provide to its subscribers. Then, we will examine the effect of various parameters (e.g., signal power and noise level) on the capacity. And we close this section by fitting our data for the received signal power to compare it with the standard free-space-loss model.

Histograms for upstream and downstream capacity are shown in Fig. 1a and Fig. 2b, respectively. A bin represents the number of users within a specific capacity range in both histograms. The aggregate number of users is normalized so that bins heights sum to 1. It is evident by the histograms that both upstream and downstream capacities are skewed-left distributions, i.e., the majority of subscribers exist on the higher

capacity. More than 80% of the subscribers fall into the interval (70 to 140) Mbps, as shown in **Fig. 2c**. On the other hand, **Fig. 2c** shows that about 90% of the subscribers fall into that interval.

To better understand the capacity distribution, we present box plots in **Fig. 2c** to visualize the quartiles of the upstream and downstream capacity data. Before we comment on Figure 1c, please note that the ISP statically preconfigured the channel capacity to be fixed at 20 MHz at the network setup time and evenly shared between the upstream and downstream for all subscribers who connect to the same AP in a tower. Comparing the two box plots, we see that the highest and lowest capacity for both downstream and upstream are almost equal. The medians also are about 90 Mbps in both cases. However, the interquartile ranges differ slightly. For the upstream, the interquartile range spans from 65 Mbps to 120 Mbps. While for the downstream, the interquartile range runs from 65 Mbps to 135 Mbps, making it 15 Mbps higher.

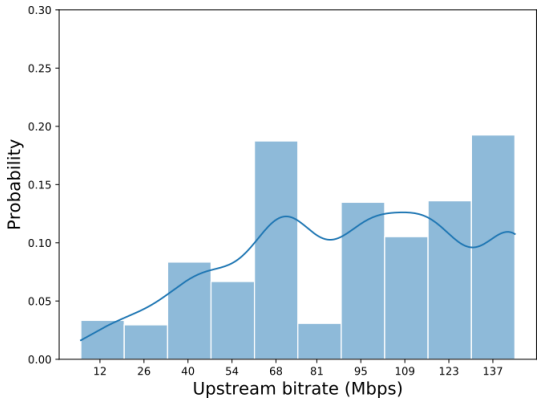

(a) Upstream capacity distribution.

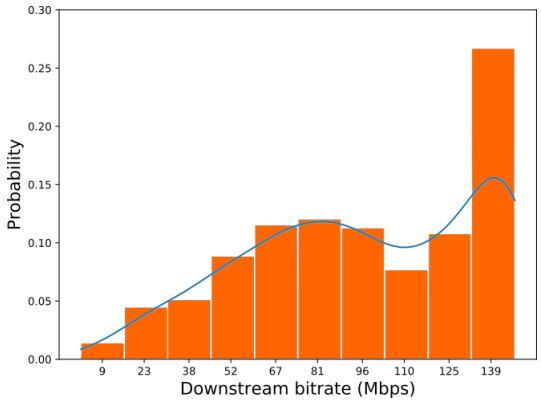

(b) Downstream capacity distribution

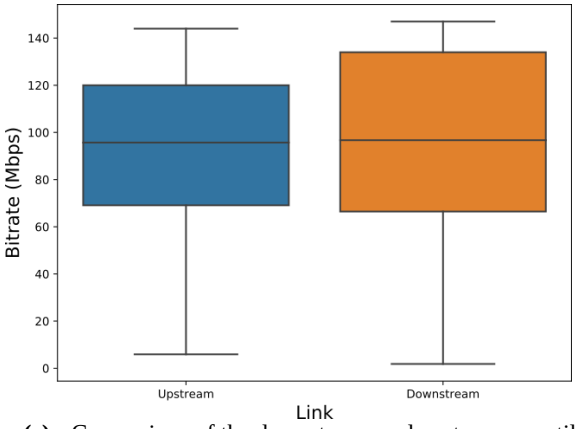

(c) Comparison of the downstream and upstream quartiles.

Fig. 2. Network users' capacity distribution.

5.1 Transmission technology

The first parameter that we explored was the effect of the transmitter technology on the maximum achievable capacity by the subscriber for both the upstream and the downstream. The transmission technology usually is specified by the equipment model. As we saw in **Table 1** and **Table 2** the details of this specification for both AP and CPE were used in the real network at the time of dataset compilation. The bar chart in **Fig. 3** shows that Multi-Input-Multi-Output (MIMO) technology provides (about twice) higher capacities for up and down streams than Single-Input-Single-Output (SISO) technology.

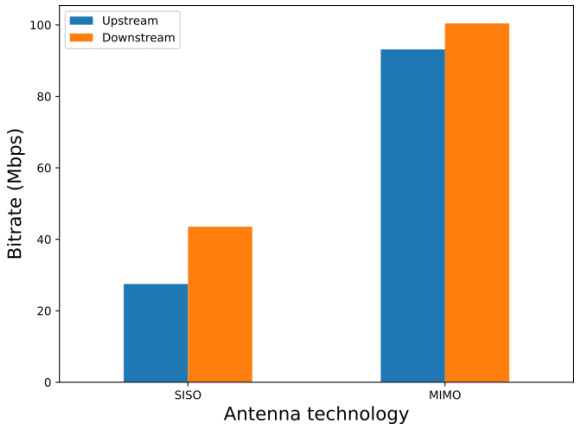

Fig. 3. The maximum achieved subscriber's capacity for both Antenna technology.

Fig. 4 shows box plots that compare the interquartile ranges for the capacity provided by the two transmitter technologies for both the upstream and downstream. Ignoring the outliers in the SISO box (**Fig. 4a**), we see that the upstream capacity does not exceed 50 Mbps, while in the case of MIMO technology, it scores up to 140 Mbps. For the downstream (**Fig. 4b**), the SISO technology can deliver up to 120 Mbps. But, 50% of subscribers using it can only get a capacity between 20 and 65 Mbps, with a median of slightly less than 40 Mbps capacity. The MIMO technology, in contrast, offers a maximum capacity of 145 Mbps and a median capacity of 100 Mbps. Compared to the SISO, about 50% of the MIMO users can get higher downstream capacity, namely in the range of 70 to 140 Mbps.

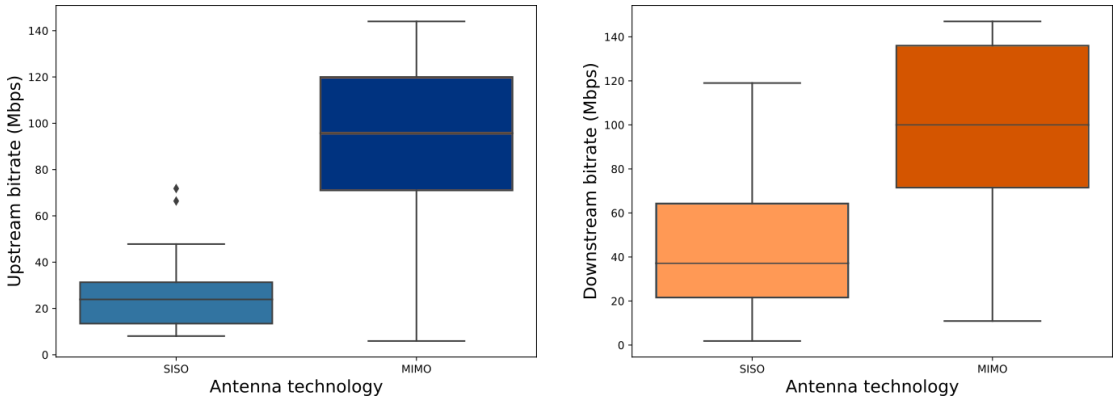

(a) Upstream Link. (b) Downstream Link

Fig. 4. The effect of the Antenna Technology on link capacity.

5.2 Modulation technique

Due to the relationship between the transmission technology and the digital modulation technique, we must also discuss the effect of the modulation technique on the capacity. Network admins often look for advanced modulation techniques in wireless digital networks to enhance the capacity to manage the limited transmission frequency spectrum problem. (The available spectrum is 20 MHz in our network). The modulation technique varies from one subscriber to another based on diverse conditions, such as the distance, the interference, and the capabilities of the subscriber's device. **Fig. 5** shows that the 16QAM technique can provide double the capacity of the QPSK technique. Also, as we move from one QAM class to the next higher one, we see a linear increase in the capacity at almost 20 Mbps. This pattern continues until the capacity hits 120 Mbps for the downstream on the 265QAM class.

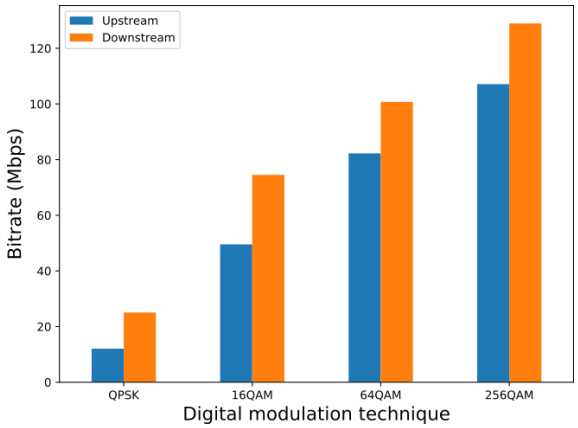

Fig. 5. The maximum subscriber's capacity achieved using different modulation techniques.

Following the same steps for examining the transmitter technology, we will now consider the box plot for the digital modulation against the upstream and downstream bit rates to understand the quartile ranges of the capacity concerning the different modulation techniques. **Fig. 6a** and **Fig. 6b** show the box plot for the modulation techniques versus upstream and downstream capacity, respectively. We can see clearly from these two figures the boost in the capacity as we move right, i.e., towards the advanced modulation technique. For instance, the 256QAM provides a median transmission capacity of 110 Mbps and 140 Mbps for the upstream and downstream links, respectively. On the other hand, the subscribers using the QPSK modulation cannot get more than 20 Mbps upstream capacity; also, 50% of the subscribers are limited in the range from 10 Mbps to 30 Mbps.

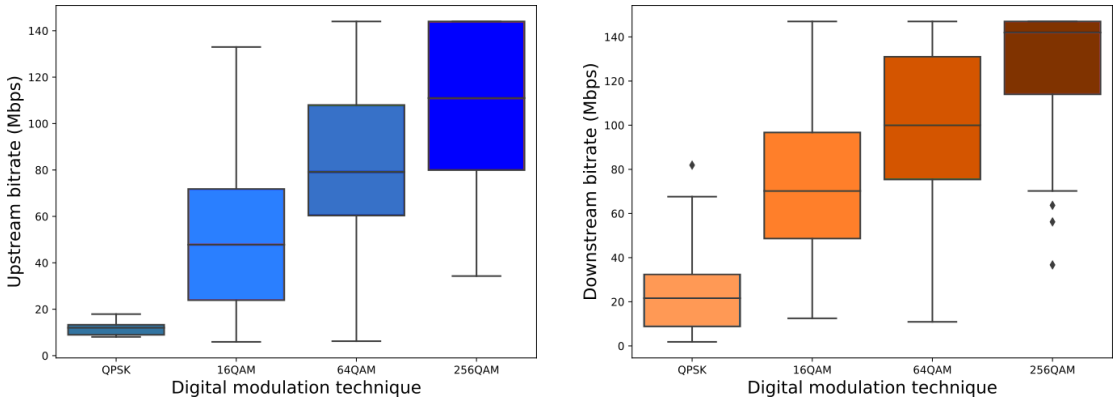

(a) Upstream Link. (b) Downstream Link

Fig. 6. The effect of various modulation techniques on the capacity.

5.3 Signal power

We can group the subscribers based on the network topology, as each group is connected to the network by one AP. Each AP operates on a specific frequency different from all other APs. The frequency varies from one AP to another, whether they exist on the same site or separate sites. APs located in far apart sites are an exception to this rule. Hence, in this case, the same frequency can be reused. **Fig. 7a** illustrates the effect of the transmitted signal power on the capacity. To model the pattern of this effect, we need to build a mathematical approximation model for those relationships. a linear model (obviously for its simplicity and popularity) has been chosen. We used the Least Squares method to build that model [35]. **Fig. 7a** Error! Reference source not found. shows a scatter plot to compare the upstream capacity against the CPE transmitted power. While **Fig. 7b** shows the scatter plot for the downstream capacity versus the CPE received power. In both cases, the fitted line shows that the capacity is directly linearly proportional to the signal power.

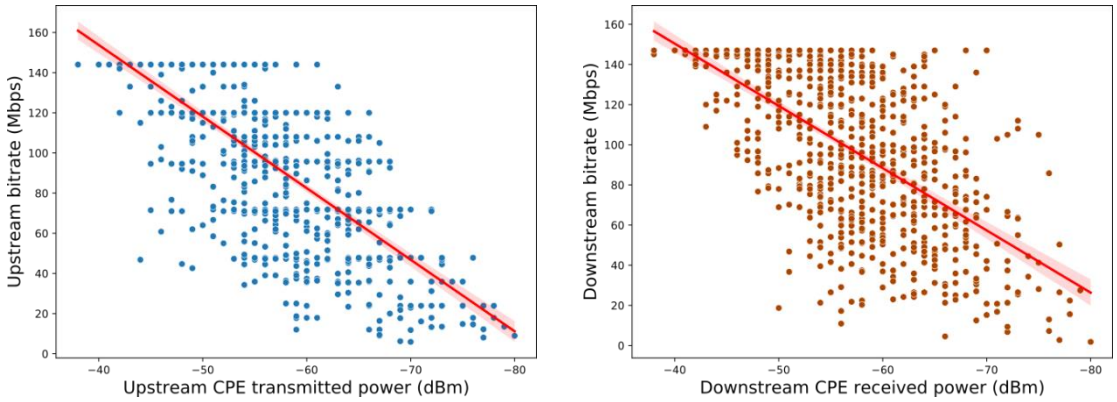

(a) CPE TX Signal power effect on the upstream capacity.

(b) CPE RX Signal power effect on the downstream capacity

Fig. 7 Capacity interpretation based on signal power.

5.4 Distance

Considering the effect of the subscriber's distance from the AP on the capacity, we see from **Fig. 8** that increasing this distance always harms the capacity. Figure 8a and Figure 8b summarize that relationship for all subscribers in our dataset and indicate that the subscriber's distance from the AP is inversely proportional to upstream and downstream capacity.

By splitting the data point based on the modulation techniques used by the subscribers for both upstream (**Fig. 8c**) and downstream (**Fig. 8d**), we find that distance has a more negative impact on the capacity obtained by the subscriber who uses the 256QAM technology. That is due to the limited power an antenna can generate and the high-power demand of the 256QAM technology to deliver such a large capacity for long distances. In general, we note that the capacity a subscriber gets from low-modulation techniques is less affected by distance. But low-modulation techniques cannot deliver high capacity. Sometimes a low-modulation may give a better capacity than a high-modulation after a certain distance, as we note in **Fig. 8c** and **Fig. 8d**. Again, that is because high-modulation techniques consume more power than low-modulation ones, and thus the reachable distances are reduced. It is worth pointing out that although the QPSK modulation is the default one for all equipment, it provides the lowest bit rate among other modulation techniques. Thus, it is technically considered useless, and there are not enough samples from which we can draw a satisfying relationship.

Since the subscribers' equipment may include various antenna technologies (because of the cost differences), we must also clarify the relationship between the capacity and the distance from the AP for the different antenna technologies. The scattered plots shown in **Fig. 8e** and **Fig. 8f** display the capacity obtained by each subscriber versus the distance from the AP for the upstream and downstream links, respectively. The yellow dots represent the MIMO antennas, while the blue dots represent the SISO antennas. The two figures emphasize the big difference in MIMO antenna users' capacity compared to SISO antenna users. All regression lines in both figures show that the capacity is inversely proportional to the distance except the line of the SISO antenna in **Fig. 8e**. We attribute this oddity to the small number of subscribers who use SISO technology since small datasets usually lead to inaccurate statistical inference.

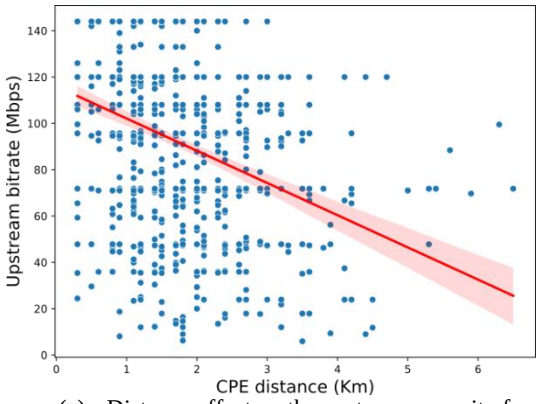

(a) Distance effect on the upstream capacity for unclassified subscribers.

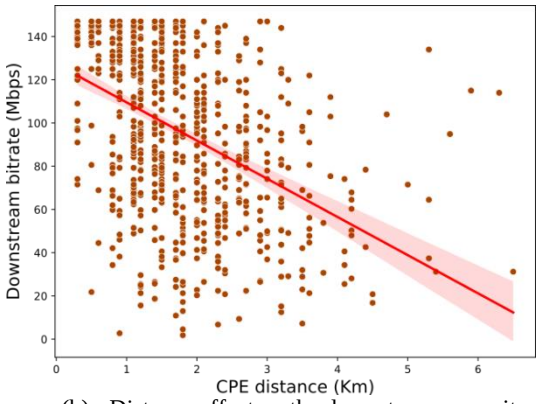

(b) Distance effect on the downstream capacity for unclassified subscribers.

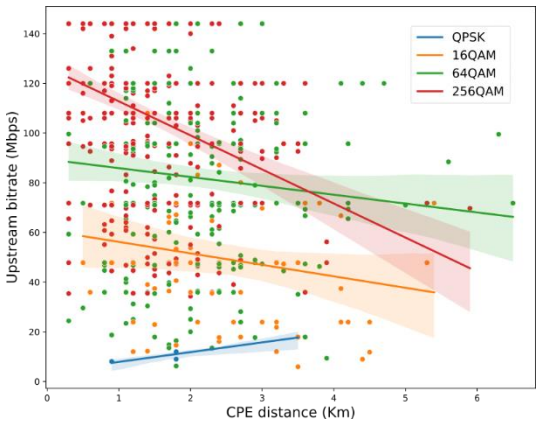

(c) Distance effect on the upstream capacity for modulation-technique's classified subscribers.

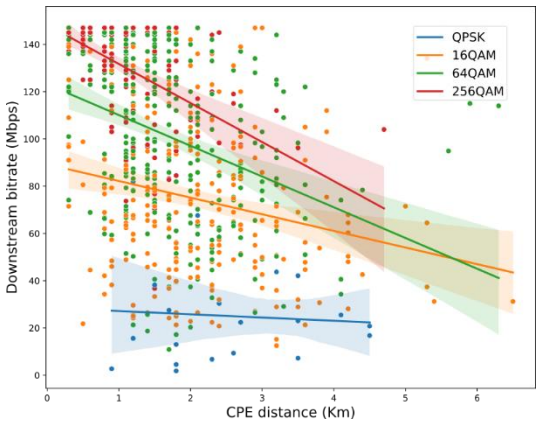

(d) Distance effect on the downstream capacity for modulation-technique's classified subscribers.

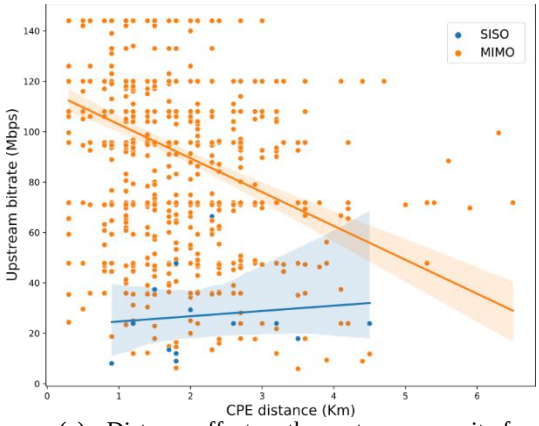

(e) Distance effect on the upstream capacity for antenna-technology's classified subscribers

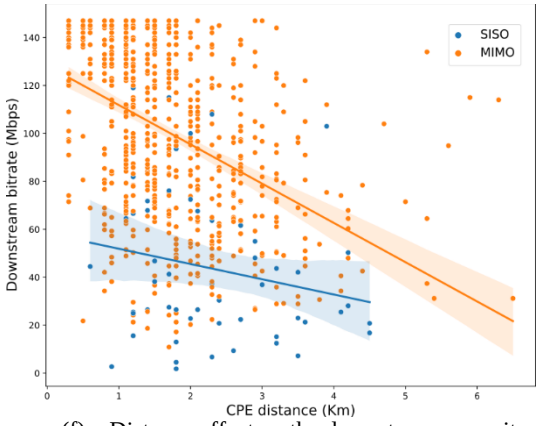

(f) Distance effect on the downstream capacity for antenna-technology's classified subscribers

Fig. 8 The relationship between the capacity and the AP-subscriber distances.

5.5 Noise

You may recall from Section 1 that the 5 GHz frequency band used by the ISPs is an open band, and there is no legalization for its use or assignment. Moreover, devices that support that frequency range are widely available in the local market at a relatively low cost. So, most, if not all, WISPs in the country use this frequency band to carry the traffic across their wireless networks. As a result, the interference must happen between the signals of the different service providers. Of course, the interference will negatively impact the quality of service, and it may occur at either end of the connection. The service provider can identify the AP which has interference through specific monitoring systems. But it is not as easy if the interference occurs at one of the subscribers' antennas. Because of this technical issue, we have been able to collect the noise data only at APs. We have classified these data into four noise levels between -125 dBm (as lower signal interference) to -65 dBm (as the very highest signal interference) received signal level at AP (as UMS describes [5]). Then, we examined the effect of each one of those noise levels on the capacity obtained by the subscriber for both upstream and downstream links.

The box plots in **Fig. 9** summarize this data. Since the interference is proportional to the ratio of the difference between the power of the original signal and the noise signal, we see in **Fig. 9a** that the effect of the interference is not significantly apparent on the upstream link; because the source of the noise in our data is not coming from the subscriber's transmitter. As mentioned above, we have collected the noise data originating from the AP transmitter. Although we thought such noise would affect the capacity of the downstream directed to the subscriber antenna, we don't see this effect clearly in **Fig. 9b**. The reason is that the service provider's monitoring of the interference helps significantly to reduce its impact. This reasoning is supported by what we observe in **Fig. 9b** of the effect of low noise on the maximum capacity that the AP can provide to its subscribers. Since the WISP often does not pay much attention to addressing the problem of low noise.

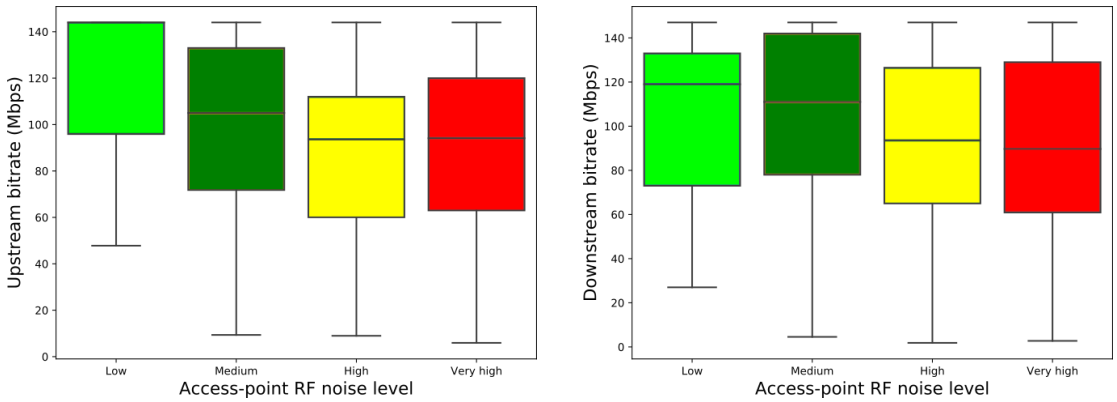

(a) Upstream links. (b) Downstream link.

Fig. 9 The effect of the AP noise level on the capacity.

5.6 PL validation

To determine whether the results obtained from this study are consistent with the standard free-space PL equation (1), we created a separate dataset for the subscribers having: the same noise environment, the same type of CPE model, and connected to the same AP model. **Fig. 10** shows a scatter plot for the dataset filtered according to these conditions and equation (2). Since we need to understand the relation between the distance and the received power at the CPE, we use a general logarithmic model (equation (3)) to fit this data. The solid curve in **Fig. 10** represents our fitted model, while the dashed one represents the general Free Space Loss (FSL) equation.

$$L_{Free\ Space} = 92.4 + 20\log f + 20\log D \quad (1)$$

$$P_{r_{CPE}} = G_{r_{CPE}} - L_{Free\ Space} + G_{t_{AP}} + P_{t_{AP}} \quad (2)$$

$$P_r = K_1 + K_2 \log D \quad (3)$$

Where:

L	Loss (dB)	P_t	Tx Power (dBm)	G_r	Rx Gain (dBi)
f	Frequency (GHz)	P_r	Rx Power (dBm)	K_1	Constant
D	Distance (Km)	G_t	Tx Gain (dBi)	K_2	Constant

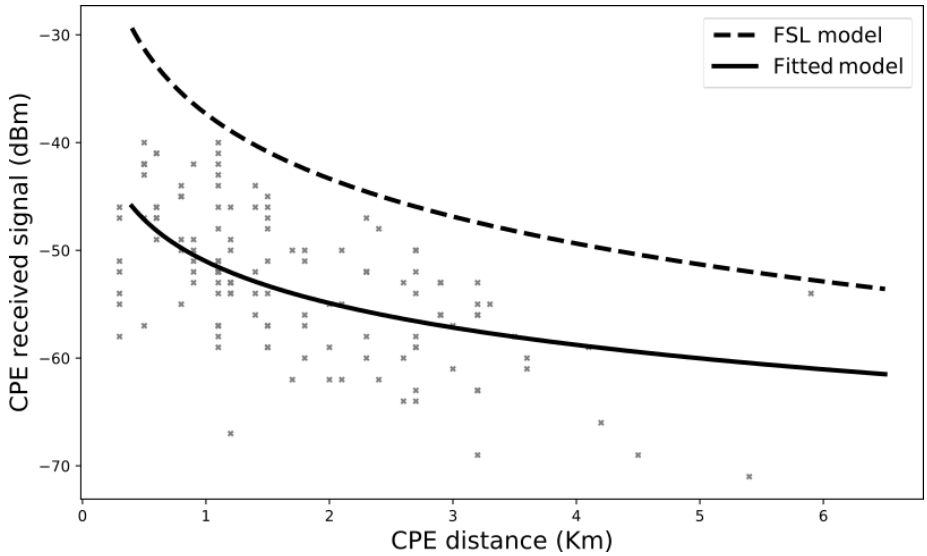

Fig. 10 CPE's received signal level vs distance.

From the curves, we can see that our fitted model follows the behavior of the FSL equation with an average of 10 dB difference, which needs more analysis in future work.

6 Conclusion

We used a statistical approach to identify the impact of many factors on the performance of an FWA network. In the studied network, since the channel width is evenly shared in both link directions, an investigation of upstream and downstream links for each CPE shows a slight boost in downstream compared to upstream. Our results reveal that network equipment that uses MIMO technology consistently provides a higher capacity to the subscriber than that uses SISO technology. Also, a higher digital modulation technique often provides a higher capacity, unless the CPE is far from the AP, the lower modulation technique tends to provide better performance because of the lower power demand by the modulation technique.

Looking at the noise effect on both the downstream and the upstream, we notice that the downstream is less affected by the noise. This state occurs because the network operator usually monitors the noise induced by the interference in the AP's surroundings. So, the operator can quickly detect that noise and fix the problem, e.g., by changing the operating frequency or adjusting the channel width. On the other hand, monitoring noise in the vicinity of CPE is not easy for the network operator; hence, he mostly depends on customer reports to detect this problem which usually leads to delays in addressing it.

Our data confirmed the linear relationship between upstream and downstream capacities on one side and the transmitted power signal on the other. Similarly, the relationship between the distance and the capacity is also linear. Finally, we compare the network PL performance extracted from our dataset against the well-known FSL model. Despite the 10 dB difference, our PL measurements still follow the behavior of the FSL model. Further investigation of this subject is needed in the future to obtain a suitable PL model that fits these results

Acknowledgment

The authors wish to thank SANA-Libya Company for sharing their network information for this work.

Conflict of Interest

This is to certify that all authors have seen and approved the manuscript being submitted and they declare no competing interest.

References

1. I. A. Alimi, R. K. Patel, N. J. Muga, and P. P. Monteiro, "Performance Analysis of 5G Fixed Wireless Access Networks with Antenna Diversity Techniques," Wireless Personal Communications, pp. 1-25, 2020.
2. P. Grønsund, P. E. Engelstad, T. Johnsen, and T. Skeie, "The physical performance and path loss in a fixed WiMAX deployment," in IWCMC, 2007.
3 Z. El Khaled, W. Ajib, and H. Mcheick, "An accurate empirical path loss model for heterogeneous fixed wireless networks below 5.8 GHz frequencies," IEEE Access, vol. 8, pp. 182755-182775, 2020.
4. V. Kiran, P. S. Telkar, D. Nayak, and D. Raj, "Wi-Fi and LTE Coexistence in Unlicensed Spectrum," in IoT with Smart Systems: Springer, 2022, pp. 773-783.
5. "Ubiquiti Inc." www.ui.com.
6. F. Idachaba, "Review of Selected Wireless System Path loss Prediction Models and its Adaptation to Indoor Propagation Environments," Lecture Notes in Engineering and Computer Science, vol. 2228, 03/15 2017.
7. A. El-Keyi, H. U. Sokun, T. N. Nguyen, Q. Ye, H. J. Zhu, and H. Yanikomeroglu, "A novel probabilistic path loss model for simulating coexistence between 802.11 and 802.15.4 networks in smart home environments," in 2017 IEEE 28th Annual International Symposium on Personal, Indoor, and Mobile Radio Communications (PIMRC), 8-13 Oct. 2017 2017, pp. 1-5, doi: 10.1109/PIMRC.2017.8292343.
8. M. Rademacher, M. Kessel, and K. Jonas, "Experimental Results For the Propagation of Outdoor IEEE802.11 Links," 2016.
9. L. Hong and Y.-W. Wu, "Path loss measurement of 2.4G band radio signal communication in disaster ruins," 2016 16th International Symposium on Communications and Information Technologies (ISCIT), pp. 439-444, 2016.
10. N. Rakesh and D. Nalineswari, "Comprehensive performance analysis of path loss models on GSM 940 MHz and IEEE 802.16 WIMAX frequency 3.5 GHz on different terrains," 2015 International Conference on Computer Communication and Informatics (ICCCI), pp. 1-7, 2015.
11. R. El Chall, S. Lahoud, and M. El Helou, "LoRaWAN Network: Radio Propagation Models and Performance Evaluation in Various Environments in Lebanon," IEEE Internet of Things Journal, vol. 6, pp. 2366-2378, 2019.
12. G. R. MacCartney and T. T. S. Rappaport, "Rural Macrocell Path Loss Models for Millimeter Wave Wireless Communications," IEEE Journal on Selected Areas in Communications, vol. 35, pp. 1663-1677, 2017.
13. G. Maurya, P. A. Kokate, S. K. Lokhande, and J. A. Shrawankar, "A Review on Investigation and Assessment of Path Loss Models in Urban and Rural Environment," IOP Conference Series: Materials Science and Engineering, vol. 225, 2017.
14. N. Moraitis, D. Vouyioukas, A. Gkioni, and S. Louvros, "Measurements and path loss models for a TD-LTE network at 3.7 GHz in rural areas," Wireless Networks, vol. 26, pp. 2891-2904, 2020.
15. K. L. Chee, A. Anggraini, and T. Kurner, "Effects of Carrier Frequency, Antenna Height and Season on Broadband Wireless Access in Rural Areas," IEEE Transactions on Antennas and Propagation, vol. 60, pp. 3432-3443, 2012.
16. M. F. D. Guzman, C. A. G. Hilario, R. V. Vistal, I. C. Mosquera, J. M. Judan, and J. J. S. Marciano, "Alternative Backhaul link for Community Cellular Network in Rural Coastal Areas," 2019 IEEE Global Humanitarian Technology Conference (GHTC), pp. 1-6, 2019.
17. S. M. Hassan et al., "Bridging the Digital Divide in Malaysia using Fixed Wireless Access," in 2021 26th IEEE Asia-Pacific Conference on Communications (APCC), 2021: IEEE, pp. 74-78.
18. N. Z. A. Rahman, K. G. Tan, T. A. Rahman, I. F. M. Idris, and N. A. A. Hamzah, "Modeling of Dynamic Effect of Vegetation for Fixed Wireless Access System," Wireless Personal Communications, vol. 96, pp. 1329-1354, 2017.
19. M. K. Adityo, M. I. Nashiruddin, and M. A. Nugraha, "5g fixed wireless access network for urban residential market: A case of indonesia," in 2021 IEEE International Conference on Internet of Things and Intelligence

Systems (IoTaIS), 2021: IEEE, pp. 123-128.
20. A. Colpaert, E. Vinogradov, and S. Pollin, "Fixed mmWave Multi-User MIMO: Performance Analysis and Proof-of-Concept Architecture," 2020 IEEE 91st Vehicular Technology Conference (VTC2020-Spring), pp. 1-5, 2020.
21. D. D. Dajab, S. E. Ogundapo, and J. Y. Oricha, "comparison of empirical and semi-empirical propagation loss models for gsm in an urban environment," 2015.
22. M. Hata, "Empirical formula for propagation loss in land mobile radio services," IEEE Transactions on Vehicular Technology, vol. 29, pp. 317-325, 1980.
23. H. Oudira, L. Diouane, and M. Garah, "Empirical Path Loss Models Optimization for Mobile Communication," in 2018 IEEE 5th International Congress on Information Science and Technology (CiSt), 2018: IEEE, pp. 443-448.
24. M. S. Mollel and M. Kisangiri, "Comparison of Empirical Propagation Path Loss Models for Mobile Communication," Computer Engineering and Intelligent Systems, vol. 5, pp. 1-10, 2014.
25. G. S. Bola and G. S. Saini, "Path Loss Measurement and Estimation Using Different Empirical Models For WiMax In Urban Area," 2013.
26. Z. Nadir and H. Al Lawati, "LTE path-loss prediction models' comparative study for outdoor wireless communications," 2018.
27. N. Moraitis, L. Tsipis, and D. Vouyioukas, Machine Learning-Based Methods for Path Loss Prediction in Urban Environment for LTE Networks. 2020, pp. 1-6.
28. Z. El Khaled, W. Ajib, and H. Mcheick, "Log Distance Path Loss Model: Application and Improvement for Sub 5 GHz Rural Fixed Wireless Networks," IEEE Access, vol. 10, pp. 52020-52029, 2022.
29. N. Z. A. Rahman, K. G. Tan, A. Omer, T. A. Rahman, and A. W. Reza, "Radio Propagation Studies at 5.8 GHz for Point-to-Multipoint Applications Incorporating Vegetation Effect," Wireless Personal Communications, vol. 72, pp. 709-728, 2013.
30. T. Schwengler and M. Glbert, "Propagation models at 5.8 GHz-path loss and building penetration," in RAWCON 2000. 2000 IEEE Radio and Wireless Conference (Cat. No.00EX404), 13-13 Sept. 2000 2000, pp. 119-124, doi: 10.1109/RAWCON.2000.881870.
31. A. L. Imoize, A. E. Ibhazeb, P. O. Nwosuc, and S. O. Ajosed, "Determination of Best-fit Propagation Models for Pathloss Prediction of a 4G LTE Network in Suburban and Urban Areas of Lagos, Nigeria," 2019.
32. S. M. Aldossari and K.-C. Chen, "Predicting the Path Loss of Wireless Channel Models Using Machine Learning Techniques in MmWave Urban Communications," 2019 22nd International Symposium on Wireless Personal Multimedia Communications (WPMC), pp. 1-6, 2019.
33. S. Worgu, S. G. Ajumo, and N. N. Odu, "Comparative evaluation of the path loss prediction performance Hata-Okumura path loss model for urban, suburban and rural areas," International Journal of Systems Science and Applied Mathematics, vol. 2, no. 1, pp. 42-50, 2017.
34. G. A. o. C. a. Informatics. " Authorized Private ISP List." General Authority of Communications and Informatics. https://www.cim.gov.ly/en/# (accessed 10/11/2022, 2022).
35. M. Merriman, A Text-book on the Method of Least Squares. J. Wiley & Sons, 1884.